Acta Materialia 102 (2016) 333–341

Contents lists available at ScienceDirect

Acta Materialia

journal homepage: www.elsevier.com/locate/actamat

Tailored thermal expansion alloys

J.A. Monroe [a], D. Gehring [a], I. Karaman [a, *], R. Arroyave [a], D.W. Brown [b], B. Clausen [b]

[a] Texas A&M University, Department of Materials Science and Engineering, College Station, TX, USA
[b] MST-8, Los Alamos National Laboratory, Los Alamos, NM, USA

ARTICLE INFO

Article history:
Received 21 June 2015
Accepted 6 September 2015
Available online 8 October 2015

Keywords:
Coefficient of thermal expansion
Negative coefficient of thermal expansion
Martensitic transformation
Shape memory alloys
Anisotropy

ABSTRACT

Current approaches to tailoring the thermal expansion coefficient of materials or finding materials with negative thermal expansion rely on careful manipulation of either the material's composition and/or the complex fabrication of composites. Here, by contrast, we report a new principle that enables the precise control of macroscopic thermal expansion response of bulk materials via crystallographic texture manipulation and by taking advantage of anisotropic Coefficients of Thermal Expansion (CTE) in a large class of martensitically transforming materials. Through simple thermo-mechanical processing, it is possible to tailor the thermal expansion response of a single material––without manipulating its composition––over a wide range of positive and negative values. We demonstrate this principle by gradually tuning the macroscopic CTE in a model NiTiPd alloy between a positive ($+14.90 \times 10^{-6}\ K^{-1}$) and a negative ($-3.06 \times 10^{-6}\ K^{-1}$) value, simply by incrementally increasing tensile plastic deformation in the martensite phase. This surprising response is linked to the large positive, $+51.33 \times 10^{-6}\ K^{-1}$, and negative, $-34.51 \times 10^{-6}\ K^{-1}$, CTE anisotropy, at the lattice level, along the different crystal directions in martensite. Similar CTE anisotropy is also shown experimentally in CoNiGa and TiNb alloys. In a model TiNb alloy, giant macroscopic CTEs of $+181 \times 10^{-6}\ K^{-1}$ and $-142 \times 10^{-6}\ K^{-1}$ are measured. A connection between the CTE anisotropy and the martensitic transformation in these and other materials systems such as NiTi, pure uranium, and $PbTiO_3$ is later made. It is shown that negative or positive thermal expansion crystallographic directions are connected to the crystallographic relationship between the austenite and martensite lattices, and can easily be predicted using the lattice parameters of austenite and martensite phases. Our current observations and analyses suggest that the tunability of the macroscopic CTE through thermo-mechanical processing is universal in materials––both ceramic and metals––that undergo martensitic transformations.

1. Introduction

Control of thermal expansion mismatch is a critical goal of engineering design in a wide range of applications, particularly in cases where system components are small, are subject to large changes (gradients) in temperatures, or require extreme dimensional stability over a wide range of temperatures. Thermal expansion compensation often requires materials with either negative or (close to) zero thermal expansion (NTE or ZTE, respectively). The most widely known mechanisms that yield negative thermal expansion (NTE) include the magneto-volume effect, atomic radius contraction upon electronic transitions and flexible networks [1]. The magneto-volume effect, first discovered in 1897 [1], is found in FeNi-based Invar alloys that are widely used for thermal expansion compensation due to its high strength and ductility. Invar's low thermal expansion originates from instabilities between different magnetic configurations that at the same time result in significant magnetostriction effects [2,3]. Recently, clear links have been made between the magneto-volume effect and the martensitic phase transformations exhibited by FeNi alloys [3,4]. In these systems, only compositional changes that affect magnetic ordering and unit cell volume can tailor Invar's thermal expansion characteristics.

Another mechanism for NTE is encountered in $Sm_{2.75}C_{60}$, one of the materials with the largest known NTE. In this case, the observed NTE arises from atomic radius contraction due to valence electron exchange. Unfortunately, this effect only occurs below 32 K [5] and is therefore of limited technological value. Other material systems exhibit NTE through atomic rotations and transverse atomic vibrations in flexible networks that occupy different atomic configurations with increasing temperature. For example, the ZrW_2O_8 [6–8] and ReO_3 families of ceramics show isotropic NTE via

* Corresponding author.
E-mail address: ikaraman@tamu.edu (I. Karaman).

http://dx.doi.org/10.1016/j.actamat.2015.09.012
1359-6454/

octahedral site rotations that cause uniform contraction in the cubic unit cell. Transverse atomic vibrations in non-cubic crystalline metal oxides (such as $Mg_2Al_4Si_5O_{18}$ cordierite [9,10], $LiAlSiO_4$ β-eucriptite [9,10], $NaZr_2P_3O_{12}$ [9,10] and $PbTiO_3$ perovskite [10]) and carbon structures [11] (such as graphite, carbon fibers and nanotubes) result in NTE in certain material directions and positive thermal expansion (PTE) in others. Unfortunately, the application potential of NTE ceramics is limited due to their low fracture toughness [12], low thermal conductivity, and the need for chemical composition changes to tailor their coefficient of thermal expansion (CTE). While carbon reinforced composites are a more attractive alternative for tailored thermal expansion compensation, harnessing carbon's low CTE requires complex and expensive composite fabrication techniques.

In this work, a new method for easily tailoring the thermal expansion coefficient of alloys that exhibit martensitic transformation by harnessing their giant NTE and PTE associated with different crystallographic directions is presented. Interestingly, the NTE and PTE directions are not solely related to the martensite's crystal symmetry, but can be predicted by comparing the high temperature austenite phase's lattice parameters with the low temperature martensite's lattice parameters. While the fundamental nature of this anisotropic thermal expansion is currently not understood, this simple correspondence successfully predicts the PTE and NTE directions of not only martensitic metals and alloys such as NiTiPd, TiNb, CoNiGa, NiTi [13], and α-Uranium [14], but also functional ceramics such as $PbTiO_3$ that undergo martensitic transformation. These different materials represent various crystallographic symmetries, composition, chemical ordering, and bonding types while sharing martensitic transformation and thermal expansion anisotropy. The ability to tailor an alloy's CTE using simple mechanical deformation promises exceptional control over thermal expansion compensation design in the automotive, aerospace, marine, electronic, power generation and transmission, and scientific instrumentation industries.

2. Experimental procedures

We selected three different alloy systems exhibiting martensitic transformation in order to demonstrate the CTE anisotropy of martensitic alloys regardless of the crystal structure of martensite, or whether the alloy is ordered or not. In addition, we show that different, but simple thermo-mechanical processing methods can be used to tailor the CTE of these alloys between large positive and large negative values, by crystallographically texturing martensite through martensite reorientation/detwinning mechanisms. These alloy systems are $Ni_{19.5}Ti_{50.5}Pd_{30}$ in polycrystalline form, $Co_{49}Ni_{21}Ga_{30}$ as single crystals, and $Ti_{78}Nb_{22}$ in polycrystalline form. Fig. 1 displays the comparison between the austenite, blue (in the web version), and martensite, green, phases for these three alloys. The three alloys were selected as representative systems to illustrate the universal nature of the CTE anisotropy and tailorable CTE in martensitic materials. Using Fig. 1, the lattice parameter correspondence between austenite and martensite will be shown to correlate with the observed thermal expansion anisotropy below.

$Co_{49}Ni_{21}Ga_{30}$ single crystal samples were grown in a He environment using the Bridgman technique. 4 × 4 × 8 mm samples were wire electro-discharge machined (EDMed) from the larger single crystals and etched to remove the EDM recast layer. The samples were then homogenized at 1473 K for 4 h, followed by water quenching (WQ) under ultra-high purity (UHP) argon in quartz ampules. These samples were mostly used for neutron diffraction experiments in order to demonstrate the CTE anisotropy in an example tetragonal ($L1_0$) martensite system. For the NiTiPd alloy, the ingots with the composition of $Ni_{19.5}Ti_{50.5}Pd_{30}$ were

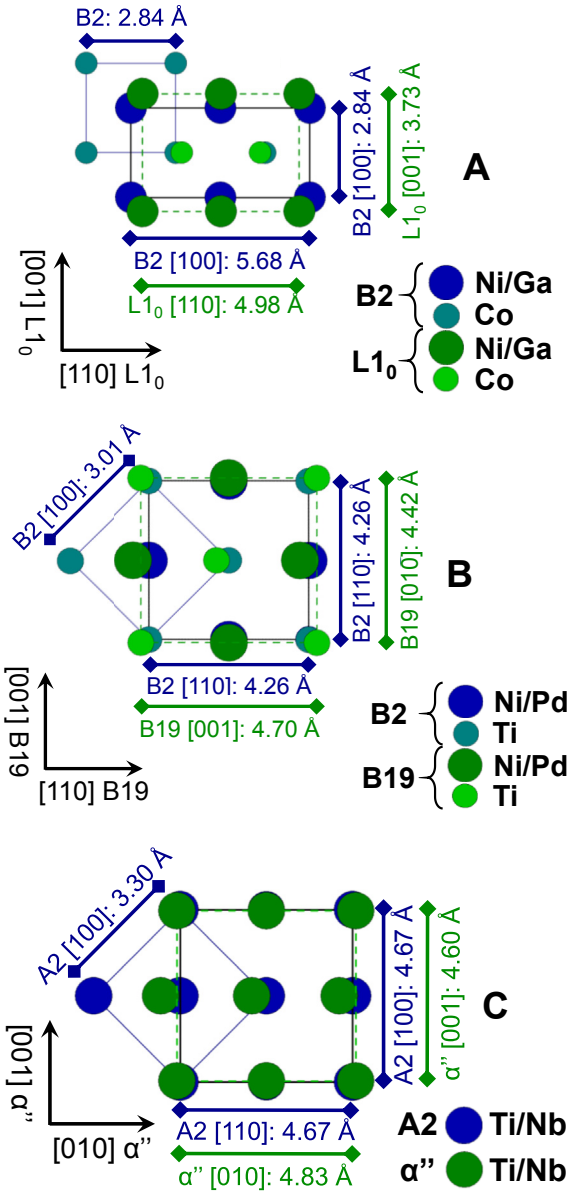

Fig. 1. Crystallographic relationships between cubic austenite (ordered B2 CoNiGa (A) and NiTiPd (B) and disordered A2 TiNb (C)), and martensite (ordered tetragonal $L1_0$ CoNiGa (A), ordered orthorhombic B19 NiTiPd (B), and disordered orthorhombic α″ TiNb (C)) of the materials studied in the present work.

vacuum induction melted in a graphite crucible and cast into a water cooled copper mold. The ingots were homogenized and encased in a steel can prior to 900 °C extrusion with a 7 to 1 reduction in area. Dog-bone tension samples were then wire EDMed from the extruded rods for tensile processing. Elemental Ti and Nb were arc melted under argon gas to obtain samples with the composition of $Ti_{78}Nb_{22}$. The ingot was then sealed in a quartz tube under UHP argon and heat treated at 1273 K for 24 h. 0.5 mm thick $Ni_{19.5}Ti_{50.5}Pd_{30}$ and $Ti_{78}Nb_{22}$ samples were wire EDM cut and polished to a mirror finish prior to the diffraction experiments.

Lattice parameters for $Ni_{19.5}Ti_{50.5}Pd_{30}$ and $Ti_{78}Nb_{22}$ were determined at discrete temperatures using X-ray diffraction (XRD), while $Co_{49}Ni_{21}Ga_{30}$ was characterized using neutron diffraction. During the diffraction experiments, all samples were first cooled to the lowest diffraction temperature and heated to each subsequent measurement temperature. XRD was conducted using Cu K-α